MAGNETIC RESONANCE IN CHEMISTRY
Magn. Reson. Chem. **36**, 496–504 (1998)

Are magic angle spinning spectra indifferent to sense of spinning?

S. C. Shekar*

Department of Molecular Biophysics and Biochemistry, Yale University, 266 Whitney Avenue, New Haven, Connecticut 06520-8114, USA

Received 8 September 1997; revised 26 December 1997; Accepted 29 December 1997

ABSTRACT: The apparent imperviousness of routine magic angle spinning (MAS) spectra to sense of spinning (clockwise/negative or counterclockwise/positive) is examined. Theoretical arguments, supported by simulations, reveal that the MAS signal depends on the spinning sense. However, this dependence is masked when appropriate symmetry of distribution of molecular orientations is present. Similar results are also found to be valid for signal arising from a 'total suppression of spinning sidebands' (TOSS) scheme. © 1998 John Wiley & Sons Ltd.

KEYWORDS: NMR; magic angle spinning; sidebands; spinning sense; total suppression of spinning sidebands

INTRODUCTION

In the field of magic angle spinning (MAS) NMR,[1–4] the tacit thought (as reflected in the body of related literature) is that the spectra are invariant to the spinning sense. In other words, it is assumed that the sideband amplitudes are the same whether one spins in a clockwise or counter clockwise fashion, for a given rate of spinning.[5]

Below it is shown that the complex sideband amplitudes do depend on both the spinning rate and sense. In fact, the sideband amplitudes for clockwise spinning are the complex conjugates of the amplitudes for counterclockwise spinning. However, for the most popular situation, that of randomly distributed orientations of the chemical shift anisotropy (CSA) tensors, it turns out that the sideband amplitudes are real and the distinction between the two possible senses of spinning disappears. Similarly, in experiments employing the 'total suppression of spinning sidebands' (TOSS) scheme,[6,7] for a 'partially' ordered system the sidebands from the two different spinning senses are complex conjugates of each other, while all the sidebands are suppressed in the case of a powder.

Observations above are strongly reminiscent of other situations wherein the symmetry of orientational distribution function (ODF)[8–11] leaves its imprint on the NMR signal (in time and/or frequency domains) of rotating solids. For example, (i) the MAS spectrum of a crystal (with the start of experiment synchronized with the same rotor position) exhibits sidebands with different phases,[4] whereas for a powder these differences disappear;[12] (ii) for a powder the spectrum acquired employing the TOSS scheme leads to a suppression of spinning sidebands, but for systems with sufficiently higher degrees of orientational order the sidebands do not vanish.[13]

* *Correspondence to*: S. C. Shekar, Department of Molecular Biophysics and Biochemistry, Yale University, 266 Whitney Avenue, New Haven, Connecticut 06520-8114, USA.

Theory

Let us consider a sample consisting of spin-$\frac{1}{2}$ nuclei rotating at magic angle with respect to the Zeeman magnetic field. We characterize this system[8–12] by a single isotropic chemical shift ω_{iso} and the CSA tensor in principal axis system (PAS), $\mathscr{A}_m^{P}$, $m = -2, 2$. Further, an orientational distribution function (ODF) characterizes the system as to whether it is a crystal (perfect order) or a powder (total disorder) or it being neither (partial order). A given orientation of the CSA tensor is uniquely specified by the triad of Euler angles[14] $\Omega \equiv (\alpha, \beta, \gamma)$, required to align the principal axis frame P with the rotor fixed frame R. The rotor fixed frame rotates about its own z-axis, and its orientation with respect to the laboratory frame (whose z-axis lies along B_0) is specified by $\Omega_{RL} = (\alpha^0_{RL} - \omega_r t, \beta_{RL}, 0)$; for exact MAS $\beta_{RL} = \arctan \sqrt{2}$. α^0_{RL} fixes the rotor position at time $t = 0$, which is defined as corresponding to the start of signal acquisition. Expanded explanations of the terminology and notation used here can be found in the literature.[11–13]

The time-dependent precession frequency associated with orientation Ω is given by,[11]

$$\omega(\Omega; \alpha^0_{RL}; \omega_r; t) = \sum_{m=-2}^{2} \omega_m(\alpha, \beta, 0) e^{im\Psi} \qquad (1)$$

where

$$\Psi = -\gamma - \alpha^0_{RL} + \omega_r t \qquad (2)$$

with the laboratory frame Fourier components of the frequency defined by

$$\omega_m(\Omega) = d^2_{m0}(\beta_{RL}) \mathscr{A}_m^{R}(\Omega) + \delta_{m,0}\omega_{iso} \qquad (3)$$

CCC 0749-1581/98/070496–09 $17.50

with

$$\mathscr{A}_m^{\mathrm{R}}(\Omega) = \sum_{m'=-2}^{2} \mathscr{A}_{m'}^{\mathrm{P}} \mathscr{D}^2_{m'm}(\Omega) \quad (4)$$

$\mathscr{A}^{\mathrm{R}}$ is the CSA tensor in the rotor frame and $\mathscr{D}^2$ and d^2 are the full and reduced Wigner rotation matrices of rank-2.[14] For MAS, $\omega_0(\Omega) = \omega_{\mathrm{iso}}$. For the remainder of discussion we set $\omega_{\mathrm{iso}} = 0$ without loss of generality.

Counterclockwise spinning

After suitably creating transverse magnetization at $t = 0$, the NMR signal at a later time owned up to by the orientation Ω is described by[8–11,13]

$$s(\Omega;\, \alpha^0_{\mathrm{RL}},\, \omega_{\mathrm{r}};\, t) = \mathrm{e}^{-Rt} f^*(\alpha,\, \beta;\, -\gamma - \alpha^0_{\mathrm{RL}}) \times f(\alpha,\, \beta;\, -\gamma - \alpha^0_{\mathrm{RL}} + \omega_{\mathrm{r}} t) \quad (5)$$

with

$$f(\alpha,\, \beta;\, \Psi) = \mathrm{e}^{i\xi(\alpha,\beta;\Psi)} \quad (6)$$

and

$$\xi(\alpha,\, \beta;\, \Psi;\, \omega_{\mathrm{r}}) = \sum_{m=0} \frac{\omega_m(\alpha,\, \beta,\, 0)}{im\omega_{\mathrm{r}}} \mathrm{e}^{im\Psi} \quad (7)$$

Equations (6) and (7) reveal that ξ is periodic in $0 \leqslant \Psi \leqslant 2\pi$ and that f inherits the same trait. This enables us to expand f as a complex Fourier series:

$$f(\alpha,\, \beta;\, \Psi) = \sum_{k=-\infty}^{\infty} C_k(\alpha,\, \beta;\, \omega_r) \mathrm{e}^{ik\Psi} \quad (8)$$

with

$$C_k(\alpha,\, \beta;\, \omega_{\mathrm{r}}) = \frac{1}{2\pi} \int_0^{2\pi} d\Psi \mathrm{e}^{-ik\Psi} \mathrm{e}^{i\xi(\alpha,\beta;\Psi;\omega_{\mathrm{r}})} \quad (9)$$

Above, a simple exponential decay characterized by a rate constant $R = 1/T_2$, with T_2 specifying the transverse relaxation time, has been assumed. Using Eqn (8) in Eqn (5):

$$s(\Omega;\, \alpha^0_{\mathrm{RL}},\, \omega_{\mathrm{r}};\, t) = \mathrm{e}^{-Rt} \sum_{k=-\infty}^{\infty} a_k(\Omega;\, \alpha^0_{\mathrm{RL}};\, \omega_{\mathrm{r}}) \mathrm{e}^{ik\omega_{\mathrm{r}} t} \quad (10)$$

where

$$a_k(\Omega;\, \alpha^0_{\mathrm{RL}};\, \omega_{\mathrm{r}}) = \mathrm{e}^{ik(-\gamma-\alpha_{\mathrm{RL}}{}^0)} C_k(\alpha,\, \beta;\, \omega_{\mathrm{r}}) \times \sum_{l=-\infty}^{\infty} \mathrm{e}^{-il(-\gamma-\alpha_{\mathrm{RL}}{}^0)} \times C_l{}^*(\alpha,\, \beta;\, \omega_{\mathrm{r}}) \quad (11)$$

Fourier series coefficients are independent of γ; the γ dependence of s is entirely contained in the oscillatory exponentials. From the above equation, the following property emerges:

$$s(\Omega;\, \alpha^0_{\mathrm{RL}},\, t + n\tau_{\mathrm{r}}) = s(\Omega;\, \alpha^0_{\mathrm{RL}},\, \omega_{\mathrm{r}};\, t)\mathrm{e}^{-Rn\tau_{\mathrm{r}}};\quad n = 0,\, 1,\, 2,\, \ldots \quad (12)$$

with the rotor period given by

$$\tau_{\mathrm{r}} = \frac{2\pi}{\omega_{\mathrm{r}}} \quad (13)$$

The immediate implication of Eqn (12) is that a Fourier transform of Eqn (10) with respect to t yields a frequency domain spectrum containing a centerband at ω_{iso} flanked on either side by an infinite set of sidebands with a uniform spacing of ω_{r}:

$$S(\Omega;\, \alpha^0_{\mathrm{RL}},\, \omega_{\mathrm{r}};\, \omega) = \sum_l a_l(\Omega;\, \alpha^0_{\mathrm{RL}};\, \omega_{\mathrm{r}}) \mathscr{L}(\omega - l\omega_{\mathrm{r}}) \quad (14)$$

where the complex Lorentzian is given by

$$\mathscr{L}(\omega) = \frac{1}{R + i\omega} \quad (15)$$

The real part of $\mathscr{L}$ is the absorption lineshape while the imaginary part is dispersive. Equation (14) drives home the point that in general dispersive and absorptive characters are mixed into the lineshape of each sideband.

By inspection, from Eqn (14), the complex sideband amplitudes are $a_k(\Omega;\, \alpha^0_{\mathrm{RL}};\, \omega_{\mathrm{r}})$, whose dependence on ω_{r} and Ω is given by Eqn (11).

Thus, the MAS spectrum is characterized by the set of complex sideband amplitudes.

Now, what would be the effect of reversing the spinning sense on the spectrum? This is the topic of the following subsection.

Clockwise spinning

At first glance, from Eqn (14), one might expect a dramatic reflection of the sideband pattern about the centerband as reflected by the change $\mathscr{L}(\omega - l\omega_{\mathrm{r}}) \rightarrow \mathscr{L}(\omega + l\omega_{\mathrm{r}})$ as the sideband enumerating subscript is left unchanged.

Figures 1 and 2 show MAS simulations of a crystal spinning, at a rate of 0.8 kHz, counterclockwise and clockwise, respectively. All other simulation parameters are identical: α, β and γ are 76.1, 52.8 and 134.9°, respectively; $\mathscr{A}_0{}^{\mathrm{P}} = 3$ kHz, $\eta = 0.5$, $R = 10$ Hz, spectral width $= \pm 15$ kHz and number of data points = 8 K. The real parts of the spectra are displayed in Figs 1(a) and 2(a) and the imaginary parts in Figs 1(b) and 2(b).

One notices that (i) the sideband pattern is indeed different for the two different senses of spinning and (ii) the difference is not the dramatic and obvious reversal of the entire sideband pattern about the centerband, (iii) but the difference is more intriguing. *Every* sideband of the counterclockwise spinning is related by a symmetry to the *same* sideband of the clockwise spinning: in the *real* part of the spectrum each sideband is *reflected* about an axis parallel to the y-axis and passing through $\omega = \omega_{\mathrm{iso}} - l\omega_{\mathrm{r}}$; in the *imaginary* part of the spectrum each sideband is *inverted* about $\omega = \omega_{\mathrm{iso}} - l\omega_{\mathrm{r}}$.

A more careful inspection of Eqn (14) exposes the fallacy of the reasoning that led to an expectation of the reversal of the entire sideband pattern about the centerband; the dependence of $a_k(\Omega;\, \alpha^0_{\mathrm{RL}};\, \omega_{\mathrm{r}})$ on ω_{r} was not taken into account. It is well known in the literature

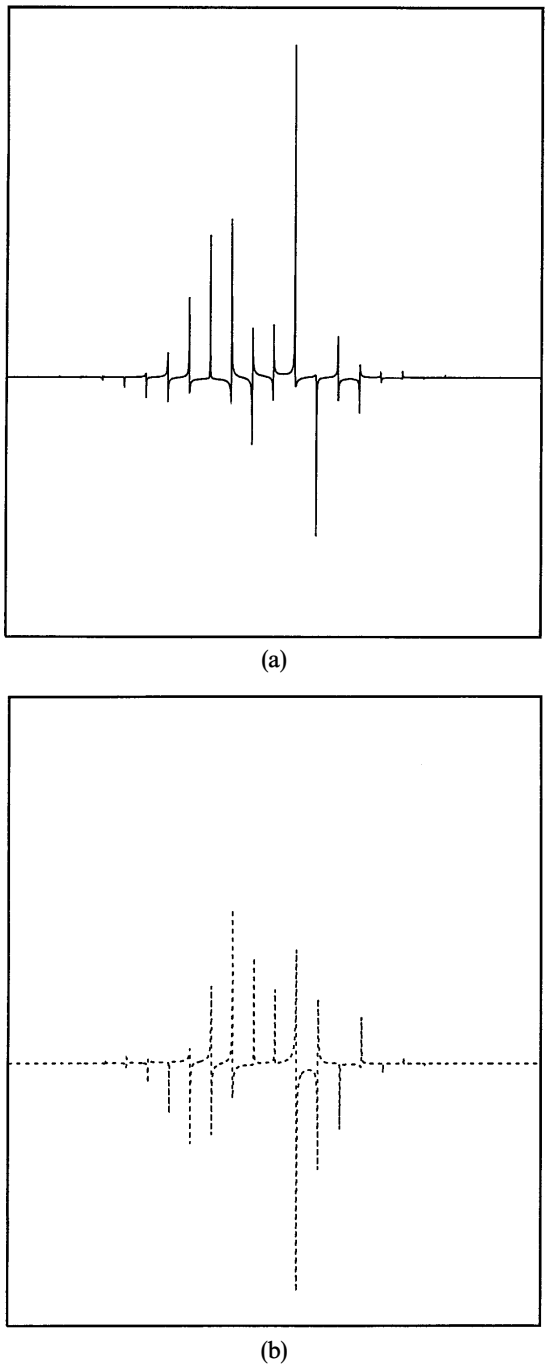

Figure 1. MAS simulations of a crystal spinning counter-clockwise at a rate of 0.8 kHz. $\mathscr{A}_0{}^P = -3$ kHz and $\eta = 0.5$ characterize the CSA tensor in the principal axis system; Euler angles from the principal axis system to the rotor system, α, β and γ, are 76.1, 52.8 and 134.9°, respectively (see text). Linewidth $R = 10$ Hz, spectral width = ± 15 kHz and number of data points = 8 K. (a) Real and (b) imaginary parts of the spectrum.

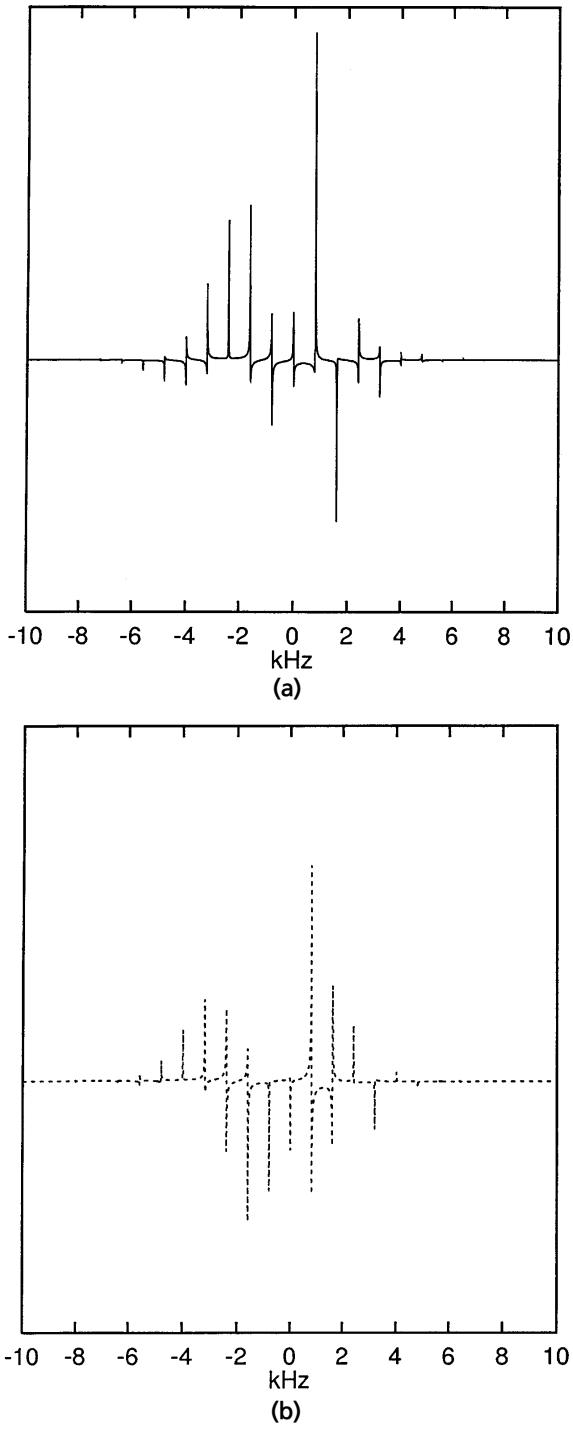

Figure 2. MAS simulations of a crystal spinning clockwise at a rate of 2 kHz. Remaining parameters as in Fig. 1. (a) Real and (b) imaginary parts of the spectrum.

that the complex sideband amplitudes do depend on the *ratio* of the principal value of the CSA tensor ($A_0{}^P$), and ω_r. In contrast, here it is pointed out that the *sign* of ω_r is also important.

The above symmetry properties will be derived after we establish the effect of change of sign of ω_r on the function ξ [Eqn (7)]. For a given orientation of the crystal α, β, γ and for a given α^0_{RL} we have the following set of relations:

$$\xi(\alpha, \beta, \gamma, \alpha^0_{RL}, -\omega_r, t) = \xi(-\alpha, \beta, -\gamma, -\alpha^0_{RL}, \omega_r, t) = -\xi(\alpha, \beta, \gamma, \alpha^0_{RL}, \omega_r, -t) \quad (16)$$

The last equality is due to Levitt,[12] from which it follows that

$$S(\Omega; \alpha^0_{RL}, -\omega_r; \omega) = \sum_k a_k{}^*(\Omega; \alpha^0_{RL}; \omega_r)\mathscr{L}(\omega - k\omega_r) \quad (17)$$

Symmetry relationships amongst spectra from spinning in opposite senses

Figure 3(a) [sum of Figures 1(a) and 2(a)] and Fig. 3(b) [sum of Figs 1(b) and 2(b)] graphically display the sum of Eqns (14) and (17):

$$S(\Omega; \alpha^0_{RL}, \omega_r; \omega) + S(\Omega; \alpha^0_{RL}, -\omega_r; \omega) = 2 \sum_l \{\mathrm{Re} \cdot a_l(\Omega; \alpha^0_{RL}; \omega_r)\} \mathscr{L}(\omega - l\omega_r) \quad (18)$$

Notice that the real part of the sum above is absorptive whereas the imaginary part is dispersive, as revealed by Fig. 3(a) and (b).

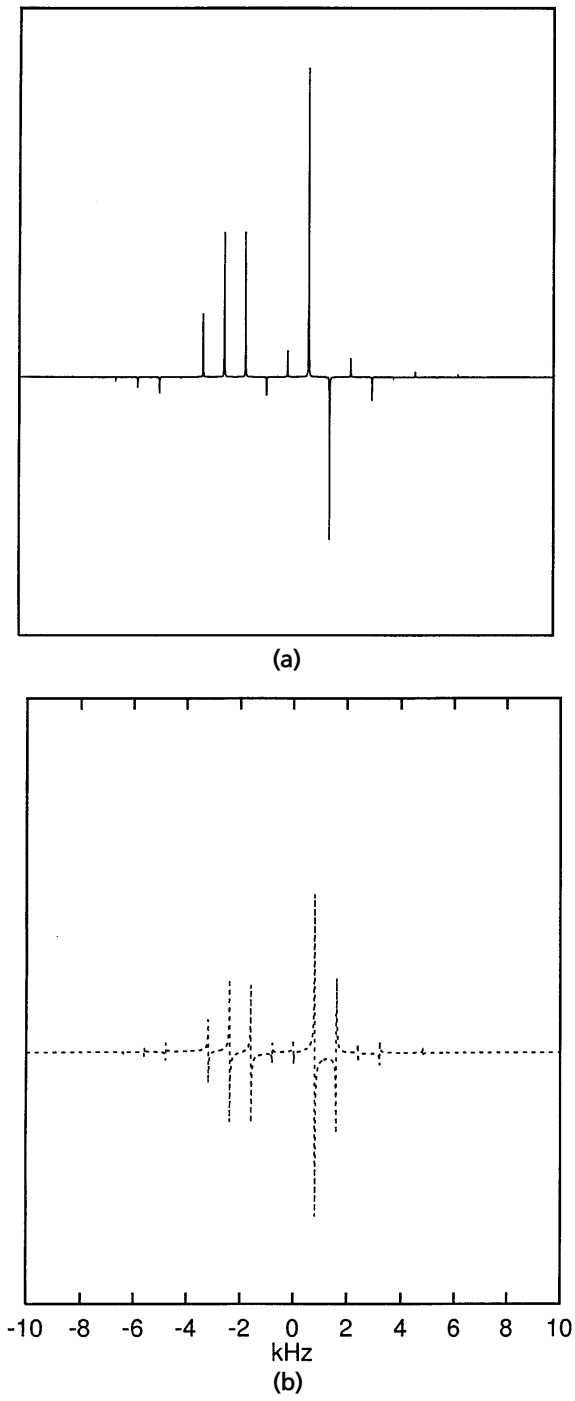

Figure 3. (a) Sum of Fig. 1(a) and (b); (b) sum of Fig. 2(a) and (b).

Next, we note the following symmetries associated with the complex Lorentzian, $\mathscr{L}(\omega)$, defined by Eqn (15): $\mathscr{L}(\omega)$ is invariant to translations along the frequency/horizontal axis; $\mathrm{Re}.\mathscr{L}(-\omega) = \mathrm{Re}.\mathscr{L}(\omega)$, symmetric in ω (invariance to reflection about the vertical axis); and $\mathrm{Im}.\mathscr{L}(-\omega) = -\mathrm{Im}.\mathscr{L}(\omega)$, antisymmetric in ω [equivalence of reflections about vertical and horizontal axes; see Fig. 4(a) and (b)], where Re. and Im. stand for real and imaginary parts, respectively.

Using the symmetries of $\mathscr{L}(\omega)$ along with Eqns (14), (15) and (17), the real and imaginary parts of the spec-

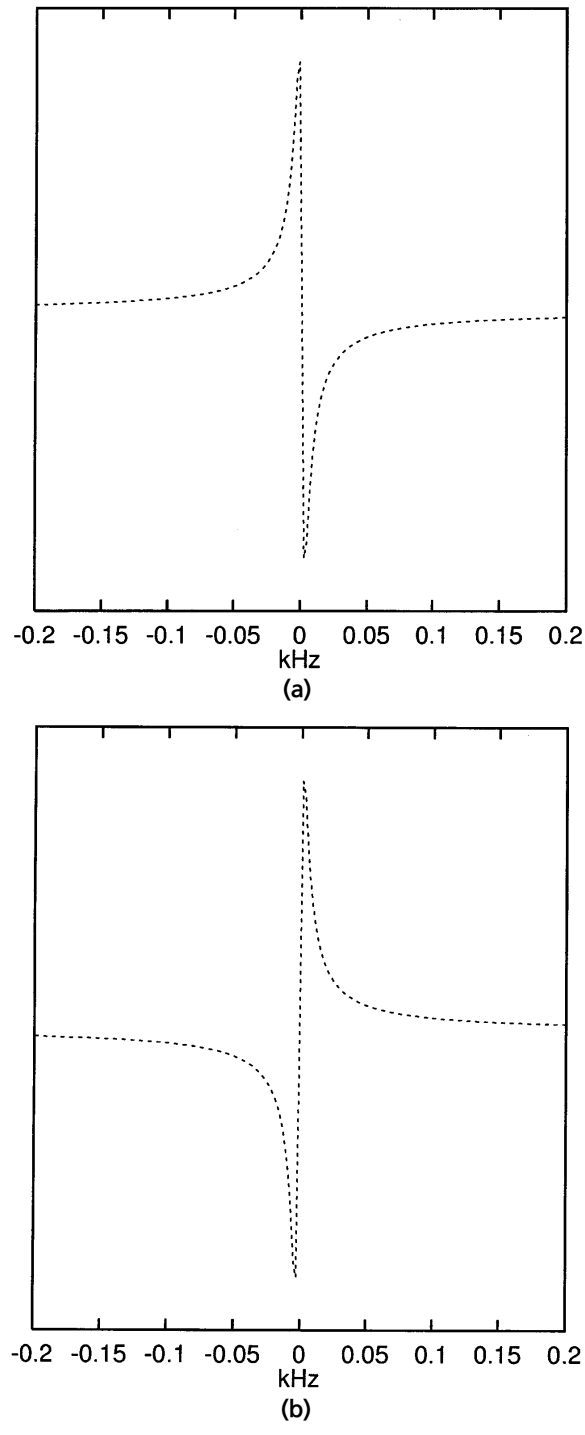

Figure 4. Imaginary parts of Lorentzians, $\mathscr{L}$ (see text), with a linewidth of 5 Hz, and centered at 0 Hz. Spectral width = 4 kHz. (a) $\mathscr{L}(\omega)$; (b) $\mathscr{L}(-\omega)$.

trum from counterclockwise (positive sense) spinning are given by

$$\begin{aligned}
&\mathrm{Re}.S(\Omega;\alpha^0_{\mathrm{RL}},\omega_r;\omega)\\
&\quad=\sum_k \mathrm{Re}.a_k(\Omega;\alpha^0_{\mathrm{RL}};\omega_r)\mathrm{Re}.\mathscr{L}(\omega-k\omega_r)\\
&\qquad-\mathrm{Im}.a_k(\Omega;\alpha^0_{\mathrm{RL}};\omega_r)\mathrm{Im}.\mathscr{L}(\omega-k\omega_r)\\
&\qquad\times\mathrm{Im}.S(\Omega;\alpha^0_{\mathrm{RL}},\omega_r;\omega)\\
&\quad=\sum_k \mathrm{Re}.a_k(\Omega;\alpha^0_{\mathrm{RL}};\omega_r)\mathrm{Im}.\mathscr{L}(\omega-k\omega_r)\\
&\qquad+\mathrm{Im}.a_k(\Omega;\alpha^0_{\mathrm{RL}};\omega_r)\mathrm{Re}.\mathscr{L}(\omega-k\omega_r)\qquad(19)
\end{aligned}$$

whereas for the clockwise (negative sense) spinning the corresponding parts are

$$\begin{aligned}
&\mathrm{Re}.S(\Omega;\alpha^0_{\mathrm{RL}},-\omega_r;\omega)\\
&\quad=\sum_k \mathrm{Re}.a_k(\Omega;\alpha^0_{\mathrm{RL}};\omega_r)\mathrm{Re}.\mathscr{L}(\omega-k\omega_r)\\
&\qquad+\mathrm{Im}.a_k(\Omega;\alpha^0_{\mathrm{RL}};\omega_r)\mathrm{Im}.\mathscr{L}(\omega-k\omega_r)\\
&\quad=\sum_k \mathrm{Re}.a_k(\Omega;\alpha^0_{\mathrm{RL}};\omega_r)\mathrm{Re}.\mathscr{L}(k\omega_r-\omega)\\
&\qquad-\mathrm{Im}.a_k(\Omega;\alpha^0_{\mathrm{RL}};\omega_r)\mathrm{Im}.\mathscr{L}(k\omega_r-\omega)\\
&\qquad\times\mathrm{Im}.S(\Omega;\alpha^0_{\mathrm{RL}},-\omega_r;\omega)\\
&\quad=\sum_k \mathrm{Re}.a_k(\Omega;\alpha^0_{\mathrm{RL}};\omega_r)\mathrm{Im}.\mathscr{L}(\omega-k\omega_r)\\
&\qquad-\mathrm{Im}.a_k(\Omega;\alpha^0_{\mathrm{RL}};\omega_r)\mathrm{Re}.\mathscr{L}(\omega-k\omega_r)\\
&\quad=-\sum_k \mathrm{Re}.a_k(\Omega;\alpha^0_{\mathrm{RL}};\omega_r)\mathrm{Im}.\mathscr{L}(k\omega_r-\omega)\\
&\qquad+\mathrm{Im}.a_k(\Omega;\alpha^0_{\mathrm{RL}};\omega_r)\mathrm{Re}.\mathscr{L}(k\omega_r-\omega)\qquad(20)
\end{aligned}$$

From Eqns (19) and (20), we can make the following observations for any given sideband. (i) The real parts of the spectra, due to a given sideband, from the two senses of spinning differ only in the sign of the $\mathrm{Im}.\mathscr{L}(\omega)$. Taking the spectrum from one sense of spinning and reversing it along the frequency axis yields the spectrum from the other sense of spinning [Figs 1(a) and 2(a)]. (ii) The imaginary parts of the spectra, of the given sideband, differ in the sign of $\mathrm{Re}.\mathscr{L}(\omega)$. This change can be accommodated by inverting the peak. However, this also inverts (reflects) $\mathrm{Im}.\mathscr{L}(\omega)$. An additional reflection along horizontal axis (the real part is unchanged) is necessary to recover $\mathrm{Im}.\mathscr{L}(\omega)$ [see Figs 1(b) and 2(b)].

Conditions for invariance of MAS spectra to spinning sense

In general, a distribution of molecular orientations is present, resulting in a distribution of CSA orientations. A given sideband is the result of contributions from all orientations, suitably weighted by the ODF. In addition, to account for accumulation of signals corresponding to a distribution of α^0_{RL} (for, e.g., signal averaging), we need to average over it as well:

$$\begin{aligned}
\langle a_k\rangle=&\int_{\alpha_{\mathrm{RL},1}{}^0}^{\alpha_{\mathrm{RL},2}{}^0}\mathrm{d}\alpha^0_{\mathrm{RL}}p(\alpha^0_{\mathrm{RL}})\\
&\times\int_0^{2\pi}\mathrm{d}\alpha\int_0^{\pi}\mathrm{d}\beta\sin\beta\\
&\times\int_0^{2\pi}\mathrm{d}\gamma p(\Omega)a_k(\Omega;\alpha^0_{\mathrm{RL}};\omega_r)\qquad(21)
\end{aligned}$$

Carousel symmetry.

$$p(\Omega)=p(\alpha,\beta)p(\gamma)=p(\alpha,\beta)\frac{1}{2\pi}\qquad(22)$$

This distribution is an important symmetry which is sufficient to ensure that all spinning sidebands have the same phase.[12] The underlying reason is that the sideband amplitudes become real. However, this also makes the distinction between spectra from opposite spinning senses disappear in accordance with Eqns (14) and (17). The real part of the spectrum shown in Fig. 5 represents this situation from *either* counterclockwise *or* clockwise spinning wherein 360 equidistant γ values between 0 and 2π have been used (the rest of the simulation parameters are the same as in Figs 1 and 2). All sidebands have the same phase. In Fig. 3(a), however, all sidebands are in an absorptive mode, and some of them are phase shifted by 180°.

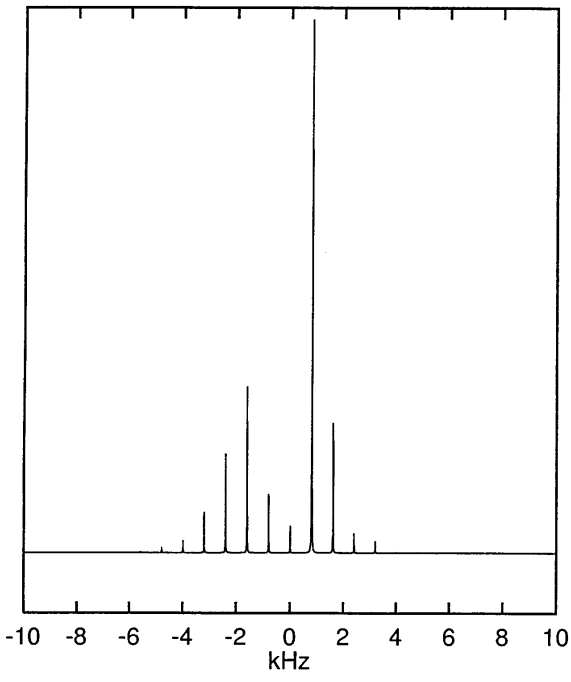

Figure 5. Real part of a simulated MAS spectrum of an ensemble of 360 crystals characterized by a uniform distribution of γ values around the spinning axis (carousel distribution; see text). The spinning sense is either counterclockwise or clockwise (the spectra are indistinguishable). Remainder of the simulation parameters as in Fig. 1.

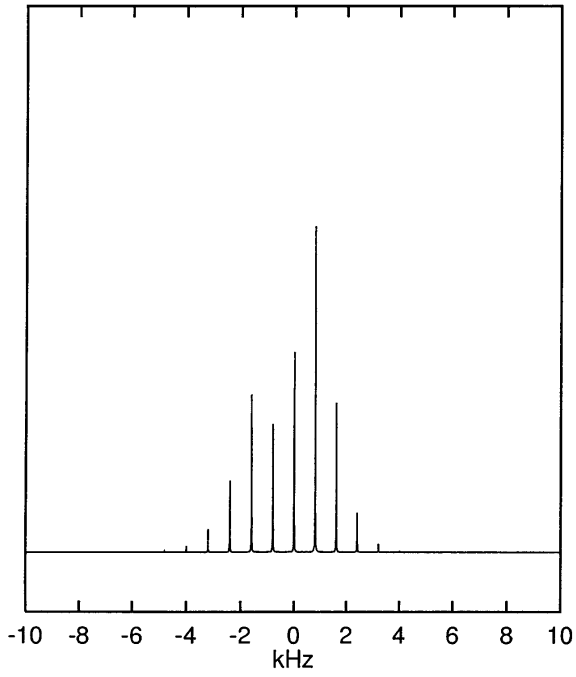

Figure 6. Real part of a simulated MAS spectrum of an ensemble of 200 000 randomly oriented crystals (powder distribution). The spinning sense is either counterclockwise or clockwise. Remainder of the simulation parameters as in Fig. 1.

Powder averages.

$$p(\Omega) = \frac{1}{8\pi^2} \tag{23}$$

This is a special case of the 'carousel' symmetry, and hence results in the invariance of the spectra to spinning sense (however, the sideband amplitudes are different in general from that of the carousel situation). Figure 6 shows the real part of the spectrum from a powder average employing 200 000 random orientations, where none of the three angles α, β, γ were held fixed; further, the spinning was *either* counterclockwise *or* clockwise (the rest of the simulation parameters are the same as in Figs 1 and 2). Once again, the sidebands are all of the same phase as in the 'carousel' situation above, but note the difference in the amplitudes from those in Fig. 5.

Unsynchronized experiments. For an unsynchronized experiment employing signal averaging (with a sufficiently large number of transients), $p(\alpha^0_{RL})$ is similar to the case of uniaxial order around the spinning axis [Eqn (22)]:[4,8–11]

$$p(\alpha^0_{RL}) = \frac{1}{2\pi}, \quad 0 \leqslant \alpha^0_{RL} \leqslant 2\pi \tag{24}$$

This situation is indistinguishable from that of the 'carousel' situation, and leads to identical time and frequency domain signals (Fig. 5).

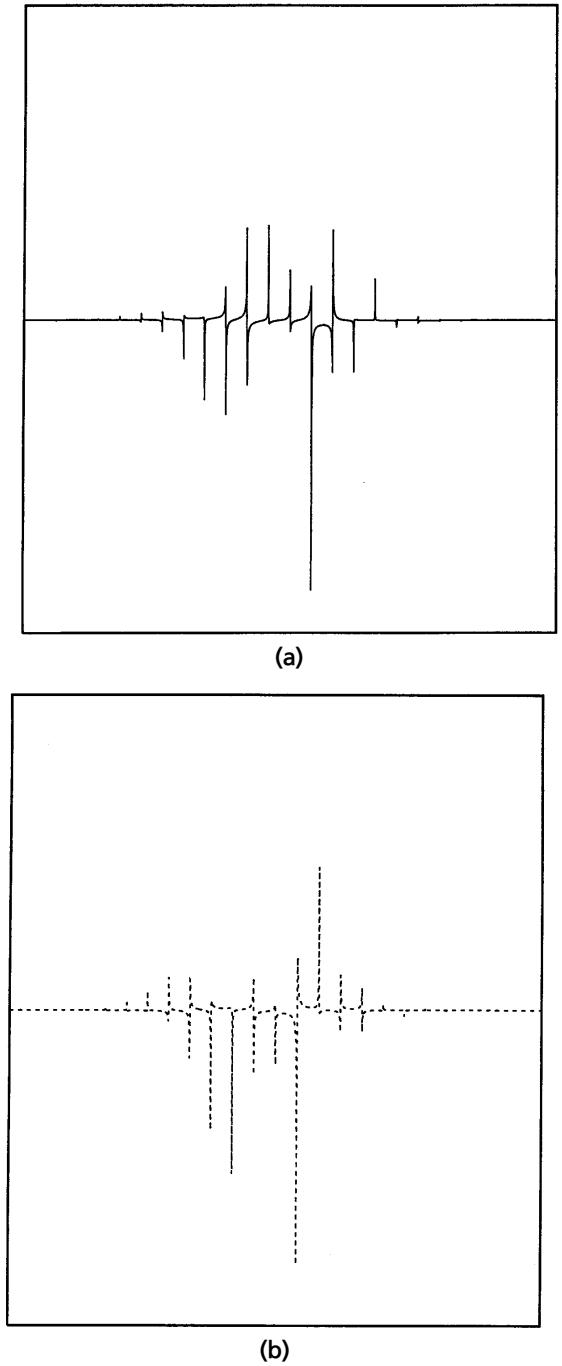

Figure 7. TOSS spectra of a crystal spinning counterclockwise. (a) Real and (b) imaginary parts of the spectrum. Simulation parameters as in Fig. 1.

TOSS

The TOSS spectrum for counterclockwise spinning has the form[11]

$$S^{TOSS}(\Omega; \alpha^0_{RL}, \omega_r; \omega) = \sum_l a_l^{TOSS}(\Omega; \alpha^0_{RL}; \omega_r)\mathscr{L}(\omega - l\omega_r) \tag{25}$$

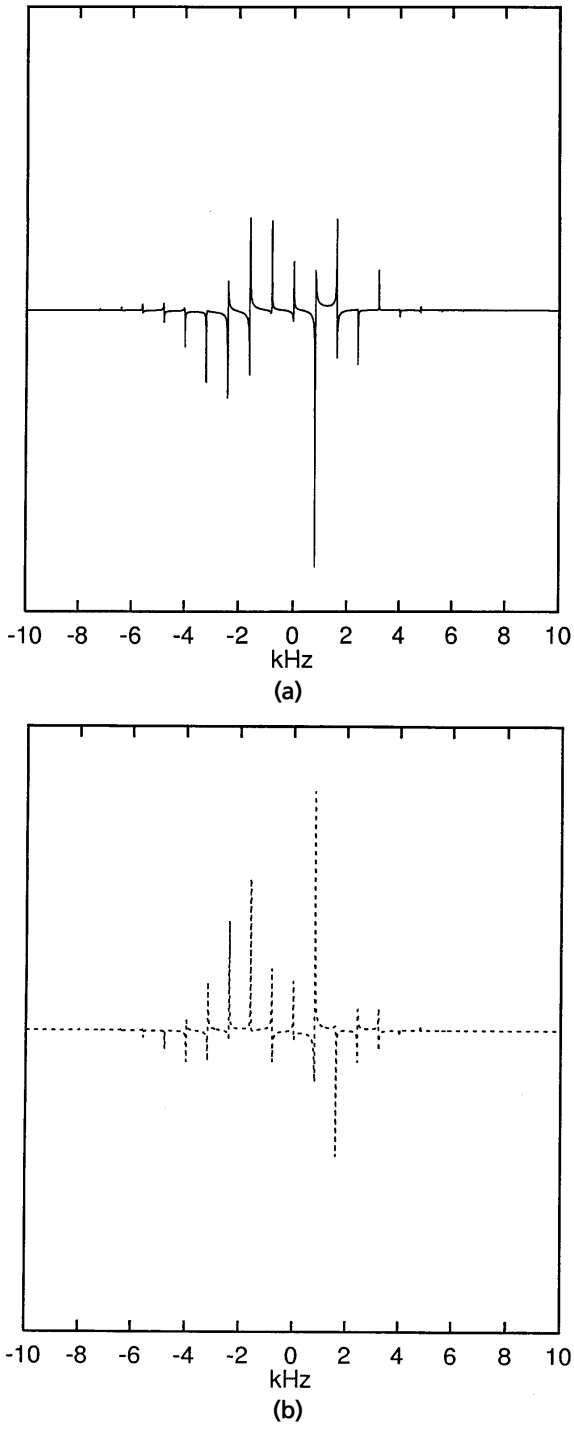

Figure 8. TOSS spectra of a crystal spinning clockwise. (a) Real and (b) imaginary parts of the spectrum. Simulation parameters as in Fig. 2.

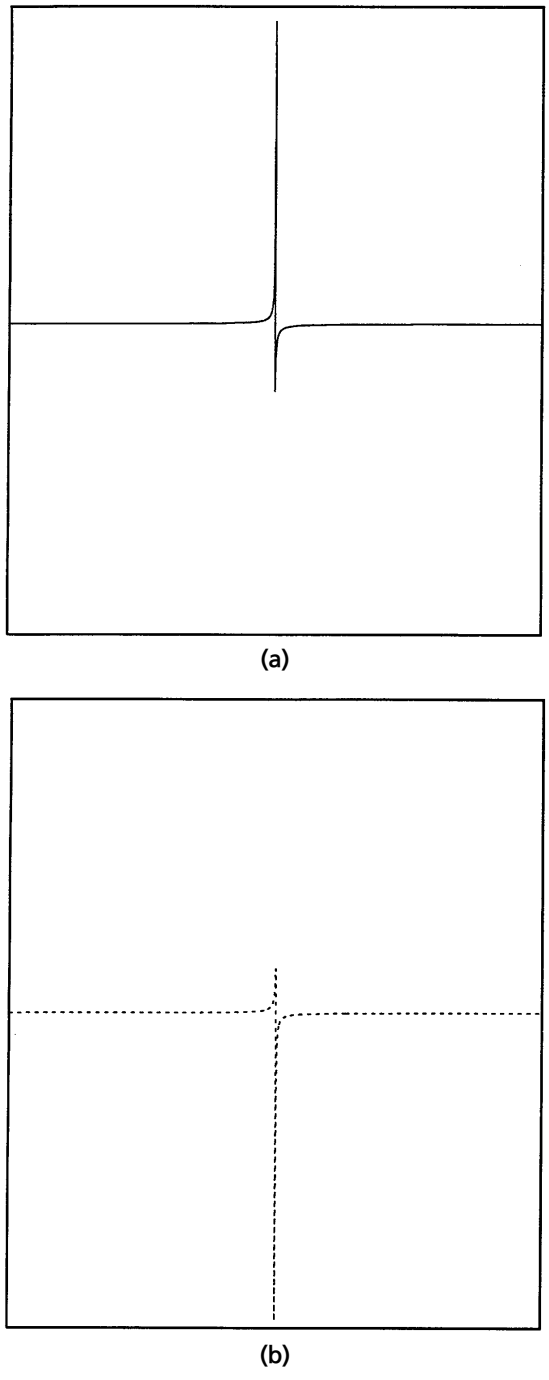

Figure 9. (a) Real and (b) imaginary parts of a simulated TOSS spectrum corresponding to anticlockwise spinning and a carousel distribution. Remainder of the parameters in Fig. 5.

where

$$a_k^{\mathrm{TOSS}}(\Omega;\ \alpha_{\mathrm{RL}}^0;\ \omega_r) = \mathrm{e}^{ik(-\gamma-\alpha_{\mathrm{RL}}{}^0)} C_k(\alpha,\ \beta;\ \omega_r) \quad (26)$$

Re-employing the reasoning presented in earlier sections, we arrive at the TOSS spectrum arising from clockwise spinning:

$$S^{\mathrm{TOSS}}(\Omega;\ \alpha_{\mathrm{RL}}^0,\ -\omega_r;\ \omega) = \sum_k a_k^{\mathrm{TOSS}*}(\Omega;\ \alpha_{\mathrm{RL}}^0;\ \omega_r)\mathscr{L}(\omega - k\omega_r) \quad (27)$$

and see that the symmetry relationships amongst the spectra from opposite senses of spinning are preserved. This is borne out by the spectra in Figs 7 and 8, which displays same symmetry relationships as in Figs 1 and 2 and as discussed above.

Now we turn our attention to the effect of symmetry of distributions on the distinction between TOSS spectra arising from opposite senses of spinning. The 'carousel' and 'powder' distributions, in addition to simulating unsynchronized experimental condition, discussed above, all lead to suppression of all sidebands for

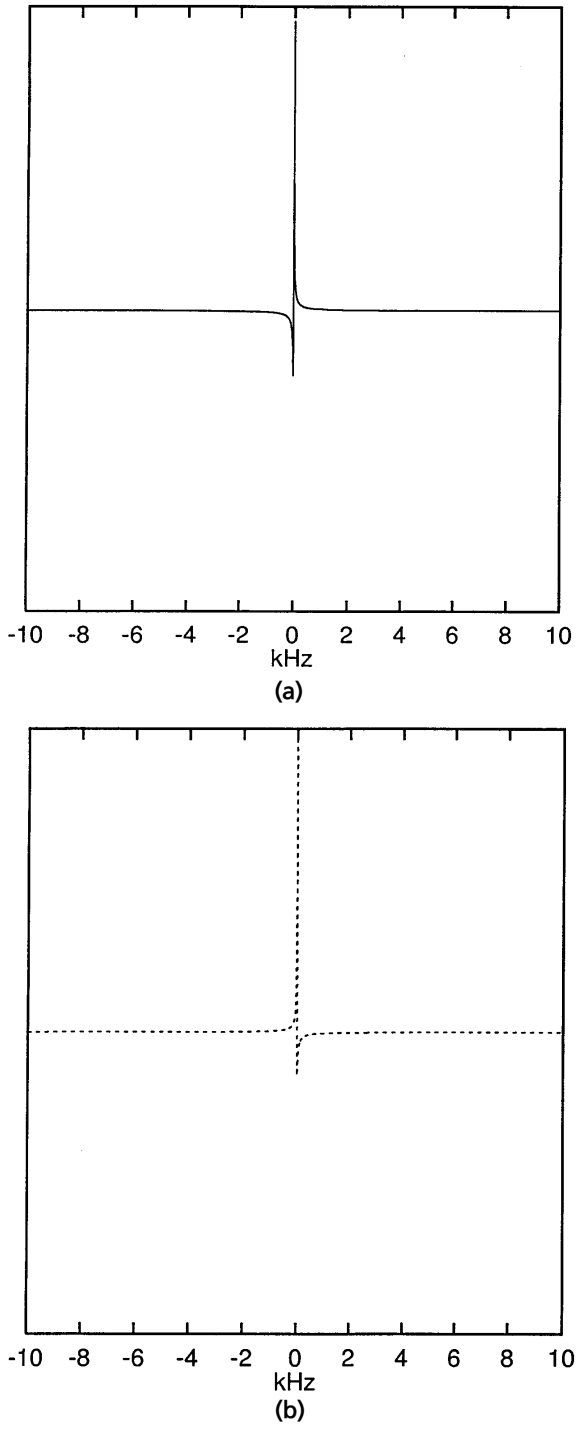

Figure 10. (a) Real and (b) imaginary parts of a simulated TOSS spectrum corresponding to clockwise spinning and a carousel distribution. Remainder of the parameters as in Fig. 6.

TOSS spectra[6,13,11] for either sense of spinning, as can be seen averaging over γ in Eqn (26). Further, for powders the residual centerbands are identical in amplitude and phase (simulations not shown), and the distinction between opposite senses of spinning totally disappears, as for MAS.

However, for carousel symmetry there is an interesting difference between TOSS and MAS cases, as far as the relationship between spectra arising from opposite senses of spinning. For MAS, there is no distinction. As theoretically predicted,[13] and experimentally fulfilled recently,[15] the centerband in TOSS can be complex in general. This can be readily appreciated by once again appealing to Eqn (26) and carrying out the requisite averaging over γ and using it in Eqns (25) and (27), whence,

$$\langle S^{\mathrm{TOSS}}(\Omega;\, \alpha^0_{\mathrm{RL}},\, \omega_r;\, \omega)\rangle_\gamma = C_0(\alpha,\, \beta;\, \omega_r)$$
$$\langle S^{\mathrm{TOSS}}(\Omega;\, \alpha^0_{\mathrm{RL}},\, -\omega_r;\, \omega)\rangle_\gamma = C_0{}^*(\alpha,\, \beta;\, \omega_r) \quad (28)$$

Figures 9 and 10 provide visual demonstration of the above relationships. The alert reader might wonder about the significance of non-reality of the centerband amplitude in TOSS as the spectrum (from either sense) can be phase corrected easily! But one would need *different* phase corrections for spectra from each spinning sense. Further, these phase corrections also differ from that of powder TOSS, powder MAS and carousel MAS cases (the last three possess same relative phase, all other things being identical). Hence only the *relative* phase of the carousel TOSS centerband with respect to the powder TOSS centerband is meaningful in practice.

CONCLUSIONS

The complex sideband amplitudes a_k, $k = -1,\ 0,\ 1$ arising from MAS are provided in Table 1 (see Figs 1, 2, 5 and 6) and the corresponding values for TOSS case are given in Table 2 (see Figs 7–10).

Spectra of samples employing magic angle sample spinning, in general, are affected by the sense of spinning. This assertion is supported by numerical simulations for the case of simple MAS experiments and also those employing a TOSS sequence (Figs 1–3, 7 and 8).

A theoretical relationship between the spectra from the two senses of spinning for both MAS and TOSS has been derived. The basic assertion is that, in both MAS and TOSS cases, the sidebands from the two senses of spinning are complex conjugates of each other, for a *single* orientation (for, e.g., a crystal) of the CSA tensor in the rotor-based frame; Eqns (14) and (17) for MAS and Eqns (25) and (27) for TOSS. Hence a theoretical framework, in which the above observations can be explained, has been provided.

The effect of the ODF pertaining to CSA tensors (and thus characterizing the degree of order present in the sample) on the relationship between the spectra from opposite spinning senses has been explored theoretically; once again the results are supported by numerical simulations. For both MAS and TOSS it is found that for powders the distinction between two spinning senses disappears. However, for a 'carousel' distribution (wherein the CSA tensors all have their z-axis at the same orientation with respect to the rotor axis), the MAS spectra are still impervious to spinning sense. On the other hand, the lone surviving centerband in TOSS (arising out of a carousel situation) in general has a complex amplitude. This results in the TOSS center-

Table 1. MAS counterclockwise and clockwise spinning sideband (center, immediate left and right) amplitudes (up to two decimal places) corresponding to a crystal (Figs 1 and 2), carousel (Fig. 6) and powder (Fig. 7)

		Sideband (Re, Im)		
Form	Spinning sense	−1	0	1
Crystal	Counterclockwise	(−0.04, 0.23)	(0.05, 0.14)	(0.66, −0.24)
	Clockwise	(−0.04, −0.23)	(0.05, −0.14)	(0.66, 0.24)
Carousel[a]		(0.05, 0.00)	(0.02, 0.00)	(0.50, 0.00)
Powder[a]		(0.12, 0.00)	(0.17, 0..00)	(0.31, 0.00)

[a] Spinning sense does not matter.

Table 2. TOSS counterclockwise and clockwise spinning sideband (center, immediate left and right) amplitudes (up to two decimal places) corresponding to a crystal (Figs 7 and 8), carousel (Figs 9 and 10) and powder (with all other parameters the same as in Fig. 7)

		Sideband (Re, Im)		
Form	Spinning sense	−1	0	1
Crystal	Counterclockwise	(0.22, −0.08)	(0.10, −0.12)	(−0.54, −0.46)
	Clockwise	(0.22, 0.08)	(0.10, 0.12)	(−0.54, 0.46)
Carousel	Counterclockwise	(0.00, 0.00)	(0.10, −0.12)	(0.00, 0.00)
	Clockwise	(0.00, 0.00)	(0.10, 0.12)	(0.00, 0.00)
Powder[a]		(0.00, 0.00)	(0.24, 0.00)	(0.00, 0.00)

[a] Spinning sense does not matter.

band amplitudes from the two spinning senses being complex conjugates of each other and the spectra obey the same symmetry relationships as for the situation of a crystal MAS or crystal TOSS.

Acknowledgements

The author thanks Professor Steven O. Smith for encouragement and support. He is deeply indebted to Professor Malcolm H. Levitt for an introduction to the magic of NMR of rotating solids and inspiring this work.

REFERENCES

1. E. R. Andrew, A. Bradbury and R. G. Eades, *Arch. Sci. Geneva* **11**, 223 (1958).
2. I. J. Lowe, *Phys. Rev. Lett.* **2**, 285 (1959).
3. E. R. Andrew, A. Bradbury and R. G. Eades, *Nature* (*London*) **183**, 1802 (1959).
4. M. M. Mariq and J. S. Waugh, *J. Chem. Phys.* **70**, 3300 (1979).
5. J. Herzfeld and A. E. Berger, *J. Chem. Phys.* **73**, 6021 (1980).
6. W. T. Dixon, *J. Chem. Phys.* **77**, 1800 (1982).
7. W. T. Dixon, J. Schaeffer, M. D. Sefcik, E. O. Stejskal and R. A. McKay, *J. Magn. Reson.* **49**, 341 (1982).
8. A. Hagemeyer, K. Schmidt-Rohr and H. W. Spiess, *Adv. Magn. Reson.* **13**, 85 (1989).
9. H. W. Spiess, *Chem. Rev.* **91**, 1321 (1991).
10. K. Schmidt-Rohr and H. W. Spiess, *Multidimensional Solid State NMR and Polymers*. Academic Press, London (1994).
11. S. C. Shekar, Z. Song, A. Rupprecht and M. H. Levitt, *Proc. Indian Acad. Sci., Chem. Sci.* **106**, 1565 (1994).
12. M. H. Levitt, *J. Magn. Reson.* **82**, 427 (1989).
13. O. N. Antzutkin, Z. Song, X. Feng and M. H. Levitt, *J. Chem. Phys.* **100**, 130 (1994).
14. M. E. Rose, *Elementary Theory of Angular Momentum*. Wiley, New York (1957).
15. O. N. Antzutkin and M. H. Levitt, *J. Magn. Reson. A* **118**, 295 (1996).

